Desalination and Water Treatment
www.deswater.com

doi: 10.5004/dwt.2017.21348

95 (2017) 9–17
November

Elaboration and characterization of ceramic microfiltration membranes from natural zeolite: application to the treatment of cuttlefish effluents

Hajer Aloulou[a], Hazem Bouhamed[b,*], Ali Ghorbel[c], Raja Ben Amar[a], Sabeur Khemakhem[a]

[a]*Laboratoire Sciences des Matériaux et Environnement, Université de Sfax, Faculté des Sciences de Sfax, Route de Soukra Km 4, 3038 Sfax, Tunisia, emails: hajer.aloulou89@yahoo.fr (H. Aloulou), benamar.raja@yahoo.com (R. Ben Amar), khemakhem_sabeur@yahoo.fr (S. Khemakhem)*
[b]*Laboratoire de Chimie Industrielle (LCI), Ecole Nationale d'Ingénieurs de Sfax (ENIS), BP 1173, 3038 Sfax, Tunisia, Tel. +216 74241403; Fax: +216 74246347; email: hazem.bouhamed@gmail.com*
[c]*Laboratoire de Chimie Hétérocyclique, Produits Naturels et Réactivité (CHPNR), Faculté des Sciences de Monastir, Avenue de l'Environnement, 5019 Monastir, Tunisia, email: ghorbelalifr@yahoo.fr*

Received 18 May 2017; Accepted 19 August 2017

ABSTRACT

Ceramic microfiltration membranes have been successfully elaborated on tubular microporous supports by slip casting process using natural Turkish zeolite mineral as the starting material. The main steps of support preparation and microfiltration layer deposition have been detailed. The tubular zeolite support sintered at 900°C for 3 h has exhibited high properties in terms of mechanical resistance, porosity and chemical stability. Scanning electron microscopy analysis has shown smooth surfaces and cracks-free membranes sintered at 850°C during 3 h. The water permeability values of the support and the membrane have been 1,218 and 534 L/h m^2 bar, respectively. The application of the microfiltration membrane to the treatment of cuttlefish effluents has confirmed good performances in terms of permeate flux and efficiency (decrease of turbidity, retention of chemical oxygen demand and total color removal).

Keywords: Membranes; Support; Separation; Filtration; Zeolite; Microstructure

1. Introduction

Membranes are widely used in several applications due to advantages offered by their relatively high stability, efficiency, low energy requirement and facility of process [1,2]. Today, various types of porous ceramic separation membranes, such as microfiltration (MF), ultrafiltration (UF) and nanofiltration are extensively studied owing to their chemical and thermal stability [3,4], good mechanical strength, pressure resistance, long working time and catalytic properties from their intrinsic nature [1], compared with organic membranes [5,6]. The commercial membranes from alumina, titania and silica are not suitable for large-scale applications because they remain too expensive from a technicoeconomic point of view [7,8]. In the last years, ceramic membranes based on natural minerals, such as clay [9], carbon [10], phosphate [11] and mineral coal fly ash [12], have increasingly attracted attention for their low cost. Other authors have prepared supports from natural non-expensive material to support the MF or UF top layer, such as graphite [13], granitic sand [14] and clay [15,16].

Zeolites are mainly composed of aluminosilicates with a three-dimensional framework structure bearing AlO_4 and SiO_4 tetrahedra. Natural zeolites have been broadly utilized due to their special physical–chemical characteristics, such as ion-exchange properties and selectivity in sorption. Furthermore, natural zeolite does not swell in water and easily forms a suspension for coating membranes on a porous support. These advantages justify the use of this mineral as the major component in the fabrication of mineral-based ceramic membranes.

* Corresponding author.

So far, most of the work has been devoted to the elaboration and characterization of ceramic membranes from commercial zeolite on alumina and mullite supports. In fact, Cui et al. [17] have prepared MF membranes on α-Al_2O_3 tube by in situ hydrothermal synthesis method, for treatment of oil contaminated water. Besides, Mastropietro et al. [18] have successfully elaborated nanozeolite membranes on porous α-Al_2O_3 tubular supports, useful in separation and catalytic contactor applications. On the other hand, Kazemimoghadam and Mohammadi [19] have prepared nanopore zeolite membranes by hydrothermal process on the surface of a porous tubular mullite support. The obtained membrane has been highly selective for permeating water preferentially with the high permeation flux in pervaporation. However, only a few reports can be found concerning zeolite membranes elaborated on natural zeolite support [20,21]. To our knowledge, no information is available on membranes elaborated on Turkish zeolite by slip casting process. In this work, we present results relative to the elaboration and the characterization of ceramic MF membranes from natural Turkish zeolite as the starting material. An investigation on the application of the obtained membranes to the treatment of cuttlefish effluents is presented.

2. Materials and methods

2.1. Preparation of the zeolite powder

Natural zeolite has been crushed and ground (planetary ball mill Retsch PM 100 at 400 rpm during 20 min) to a fine powder passing through a sieve with mesh size 100 μm.

2.2. Characterization of the zeolite powder

Natural zeolite mineral has been obtained from Turkey (Biga, Çanakkale Province). The chemical composition of the zeolite has been determined by X-ray fluorescence for metals. Phases present in the powder have been analyzed using an X-ray diffractometer (Siemens, Germany) with Cu K_α radiation (λ = 1.5406 Å) at room temperature. Infrared absorption measurements have been carried out using a Fourier transform infrared (FTIR) spectrophotometer (PerkinElmer Spectrum One) from 4,000 to 400 cm^{-1}. The thermogravimetric analysis (TGA) of the zeolite powder has been performed from the ambient temperature to 1,000°C with a rate of 10°C/min under static atmospheric conditions. Linear shrinkage has been determined by dilatometry (Setaram TMA 92 dialometer) with a heating rate of 10°C/min from the ambient temperature to 1,100°C.

2.3. Elaboration of porous zeolite support

Plastic paste has been prepared from zeolite powder mixed with organic additives as follows:

- 84 wt% of zeolite powder,
- 8 wt% of starch: porosity agent (Cerestar RG03408, Cargill, France),
- 4 wt% of amijel: binder (Cplus 12076, Cerestar),
- 4 wt% of methocel: plasticizer (The Dow Chemical Company).

For the preparation of a homogeneous paste, a quantity of 105 mL of distilled water per 200 g of the mixed powder has been added. The plastic paste has been aged for 1 d then extruded in tubular pieces of 8 mm of external diameter and 5 mm of internal diameter. The tubes have been dried at room temperature then sintered to obtain a consolidated ceramic. Fig. 1 shows the main steps of support preparation (a) and the sintering program (b). Two steps have been defined: the first for the elimination of organic additives at 300°C during 2 h and the second for the sintering at different temperatures during 3 h.

2.4. Preparation of the zeolite microfiltration layer

The active MF layer from the same natural zeolite powder used for support elaboration has been prepared by a slip casting process (closed-end tubes of 150 mm in length, with an inner diameter of 5 mm).

The optimal composition (wt%) of the deflocculated slip has been found to be:

- 5 wt% of zeolite powder (a quantity of 74 g of natural zeolite has been crushed during 40 min with the assistance of a planetary ball mill Retsch PM 100 at 400 rpm than calibrated with 63 μm),
- 30 wt% of polyvinyl alcohol (12% w/w aqueous solution),
- 65 wt% of water.

The deposition of the slip on the zeolite support has been performed by the suspended powder technique using

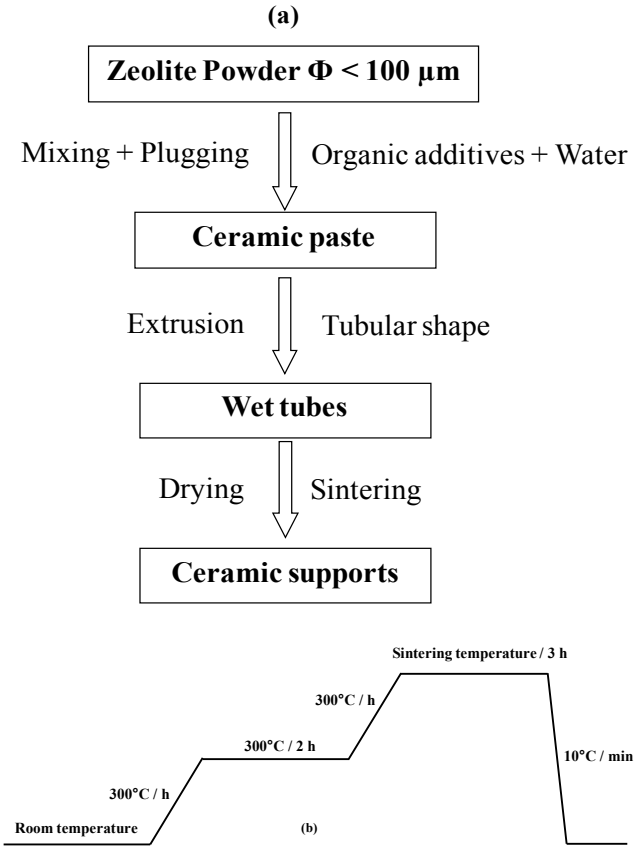

Fig. 1. Main steps of support preparation (a) and sintering program (b).

a deposition time about 7 min. After drying at room temperature for 24 h, the MF layer has been sintered at different temperatures (820°C, 850°C and 880°C) for 3 h after debonding at 250°C for 2 h.

2.5. Permeability test and mercury porosimetry

Permeability tests have been performed using a homemade pilot plant [9] at ambient temperature and transmembrane pressure (TMP) ranged between 1 and 3 bar. The flow rate has been fixed at 1.76 m/s. Before the tests, the support or the membrane has been conditioned by immersion in pure distilled water for a minimum of 24 h. The working pressure has been obtained using a nitrogen gas source. The permeability of the support has been calculated from the fluxes measured after stabilization for all working pressure. The support permeability (L_p) can be determined using the variation of the distilled water flux (J_w) with the TMP (ΔP) following the Darcy's law:

$$J_w = L_p \Delta P \text{ with } \Delta P = \left(\frac{P_{inlet} - P_{outlet}}{2} - P_f \right)$$

where P_{inlet} is the inlet pressure, P_{outlet} is the outlet pressure and P_f is the filtrate pressure.

Pore size and porosity of the samples have been measured by mercury porosimetry (mercury porosimeter Pascal 440) at high pressure (400 MPa).

3. Results and discussion

3.1. Characterization of the zeolite powder

3.1.1. Chemical composition

The chemical composition (wt%) of the zeolite powder is presented in Table 1. The major chemical components in the natural zeolite are silica (SiO_2: 73.3%) and alumina (Al_2O_3: 11.75%). The other oxides are present in very low amounts.

3.1.2. Phase identification

Fig. 2(a) shows the X-ray diffraction (XRD) pattern of the raw zeolite powder. It is clear that clinoptilolite and calcite are the main crystalline phases of the starting zeolite material. Small quantities of impurities are also present.

Table 1
Composition (wt%) of zeolite powder

SiO_2	73.3
Al_2O_3	11.75
$CaCO_3$	6.8
CaO	3.79
Fe_2O_3	1.53
K_2O	1.44
MgO	1.19
Na_2O	0.36
TiO_2	0.03
ZnO	0.01

3.1.3. FTIR spectrum

IR spectral data of the zeolite powder is shown in Fig. 3. The large bands at 3,625.45 and 3,428.57 cm^{-1} are attributed to the stretching vibrations of the OH groups of water molecules. The band at 1,638.93 cm^{-1} corresponds to the bending vibration mode of residual H_2O molecules in the zeolite voids. The absorption band at 1,202.79 cm^{-1} could be attributed to the external vibrations between SiO_4 and AlO_4 tetrahedra of the zeolite [22,23]. The internal linkages between SiO_4 and AlO_4 tetrahedra are detected at 1,059.67 cm^{-1} [24]. The low intensity bands at 790.72 and 721.67 cm^{-1} are due to the symmetrical stretching of the internal tetrahedra [25,26]. The fine bands at 674.12 and 606.59 cm^{-1} are attributed to the external linkage symmetrical stretching [26,27]. Finally, the fine and intense band at 462.56 cm^{-1} corresponds to the bending vibration Si–O [25,26].

3.1.4. Thermal analysis

The water molecules in zeolites can be classified into three groups: physisorbed water (<100°C), water associated with extra-framework cations and aluminum (100°C–400°C) and water associated with silanol nests (>400°C). Fig. 4 presents the TGA curve of natural zeolite.

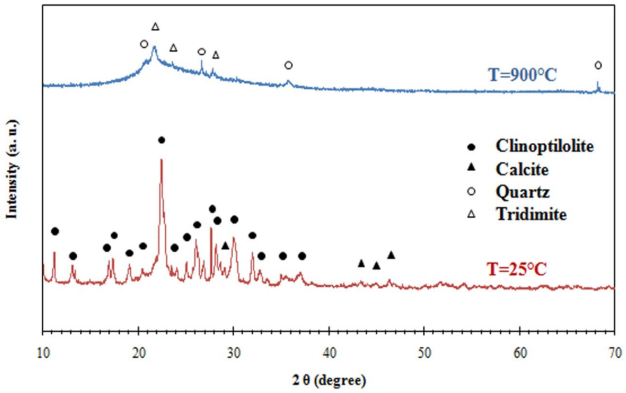

Fig. 2. XRD patterns of raw zeolite powder (a) and zeolite support sintered at 900°C during 3 h (b).

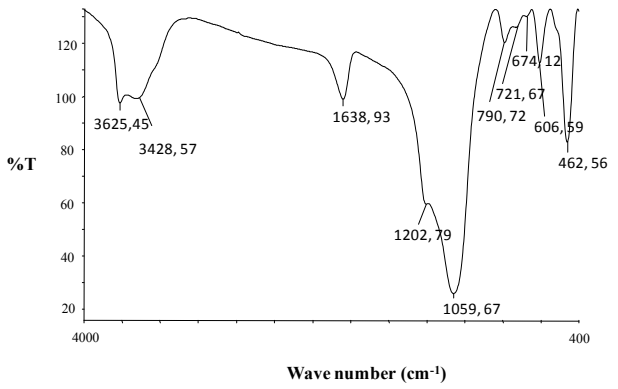

Fig. 3. IR spectrum of zeolite powder.

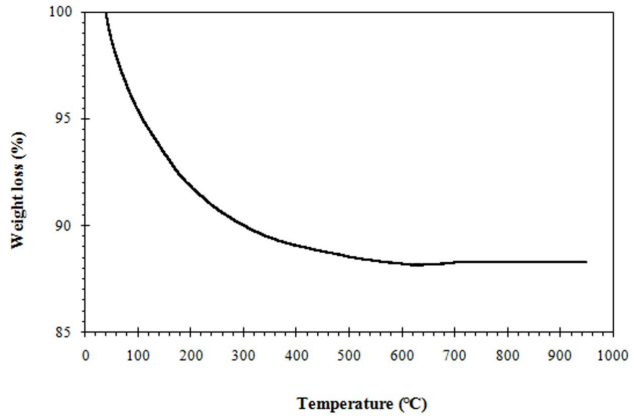

Fig. 4. Thermogravimetric analysis of zeolite powder.

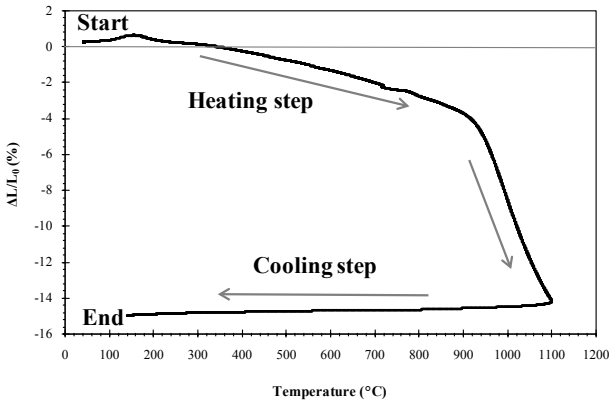

Fig. 5. Dilatometric analysis of zeolite support.

- In the temperature range 25°C–100°C, the weight loss of 4.62% is caused by the desorption of physisorbed water.
- The weight loss of 5.36% between 100°C and 300°C could be qualified the water associated with extra-framework cations and aluminum.
- Over the temperature range 300°C–600°C, the weight loss of 1.78% corresponds to the water molecules associated with silanol nests that can form strong bond interactions with water as noted by Garcia-Basabe et al. [28].
- The weight loss between 600°C and 950°C is negligible because of the removal of water associated with silanol nests.

TGA analysis has confirmed that natural zeolite used in this work is a clinoptilolite type whose structure cannot be easily broken. This high thermal stability beyond 600°C of the raw zeolite has been also demonstrated by other authors [29,30].

3.1.5. Dilatometry analysis

Dilatometry analysis has been carried out on the zeolite support used in this study to evaluate its extent of shrinkage in the temperature range from 40°C to 1,100°C (Fig. 5). During the heating process, a contraction phenomenon has been observed from 300°C to 1,100°C. At 720°C, the speed behavior has changed because of the dehydroxylation of the main components of the zeolite support. From 300°C to 900°C, the linear shrinkage has not exceeded 3.4%. The sintering process has started at about 900°C. The maximum densification speed, corresponding to the inflexion point of the dilatometric curve, has occurred at about 1,000°C. In the temperature range from 900°C to 1,100°C, the linear shrinkage has been about 10%. During the cooling step, no transformation has been detected.

3.2. Characterization of the support

3.2.1. Phase identification

From XRD analysis of the zeolite support sintered at 900°C during 3 h (Fig. 2(b)), it can be seen that the main crystalline phases are quartz and tridymite. The phase composition of the zeolite powder and the zeolite support are different due to the sintering process.

3.2.2. Scanning electron microscopy

Scanning electron microscopy (SEM) micrographs of the zeolite support sintered at 850°C, 900°C and 950°C are shown in Figs. 6(a)–(c), respectively. These micrographs reveal a good homogeneity of the surface and the absence of any cracks. The formation of grain boundaries has been achieved in this narrow temperature range. By comparing SEM micrographs between 850°C and 950°C, we note a significant evolution of the relative density of the sintered material. So, it is clear that the porosity of the zeolite support decreases with increasing sintering temperature between 850°C and 950°C. The high quality of the elaborated support with cracks-free and smooth surface would certainly contribute to an effective deposit of a selective layer.

3.2.3. Chemical resistance

The supports sintered at 850°C, 900°C and 950°C have been soaked at room temperature using HCl and NaOH solutions. The results reported in Figs. 7(a)–(c) show that zeolite supports resist better in acid medium than in basic solution. In fact, in acid medium, the weight loss does not exceed 0.42 wt% in 72 h. However, in basic solution, the weight loss reaches 1.71 wt% in 72 h for the sample sintered at 850°C. In conclusion, the weight loss has been negligible when a sample has been exposed during 3 d in basic or acid solution at the same conditions in terms of time and temperature. Results of this analysis confirm again the high quality of the elaborated zeolite supports in the temperature range from 850°C to 950°C. By comparing the chemical resistance of the samples after 72 h, we note a significant decrease of the weight loss from 850°C to 950°C in the presence of NaOH 0.5 M. The best chemical resistance in basic solution is obtained for the highest sintering temperature (0.12% for 950°C). However, in acid medium (HCl 0.2 M), the support sintered at 900°C has higher chemical resistance than the samples sintered at 850°C and 950°C. In fact, the sintering at 950°C caused a chemical degradation marked by a color change and a partial melting of residual impurities. The sample sintered at 900°C presents a total chemical resistance in acid medium/72 h and a very negligible weight loss (less than 0.6 wt%) in NaOH solution/72 h. This temperature of 900°C could be chosen as optimal sintering temperature.

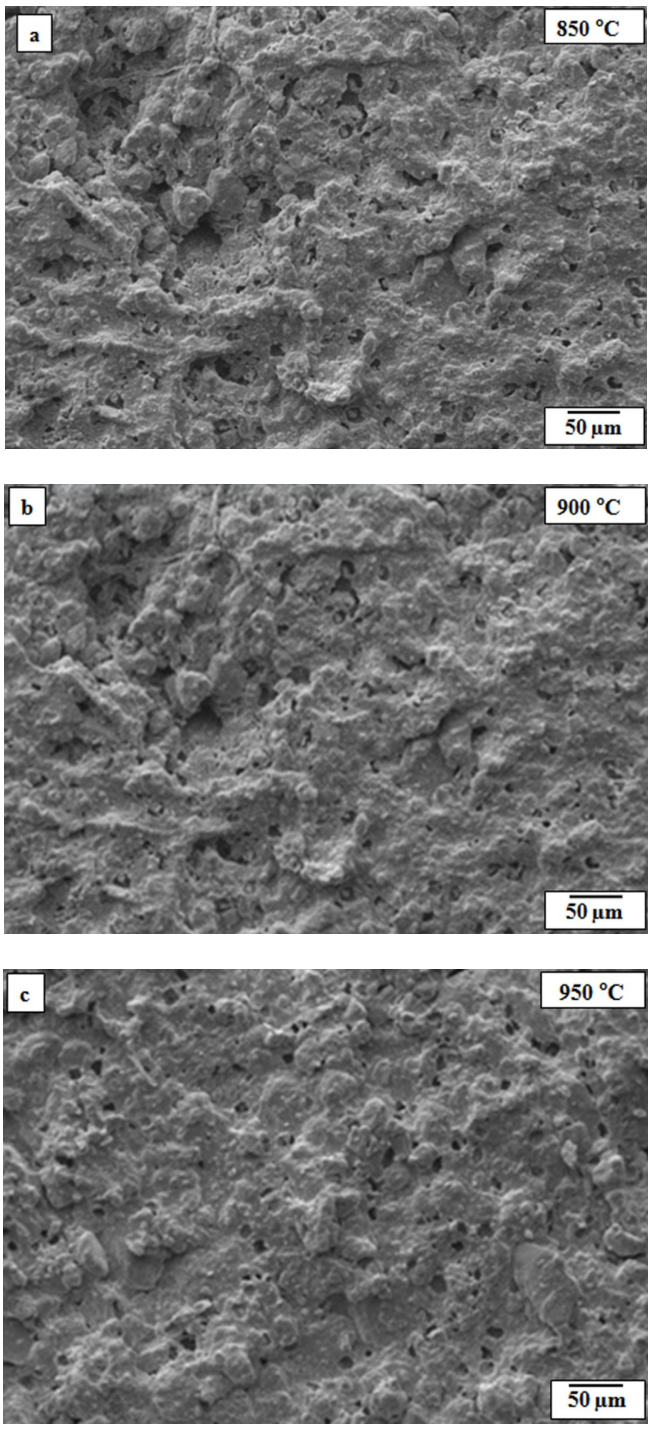

Fig. 6. SEM micrographs of internal surface of tubular zeolite support sintered at 850°C (a), 900°C (b) and 950°C (c).

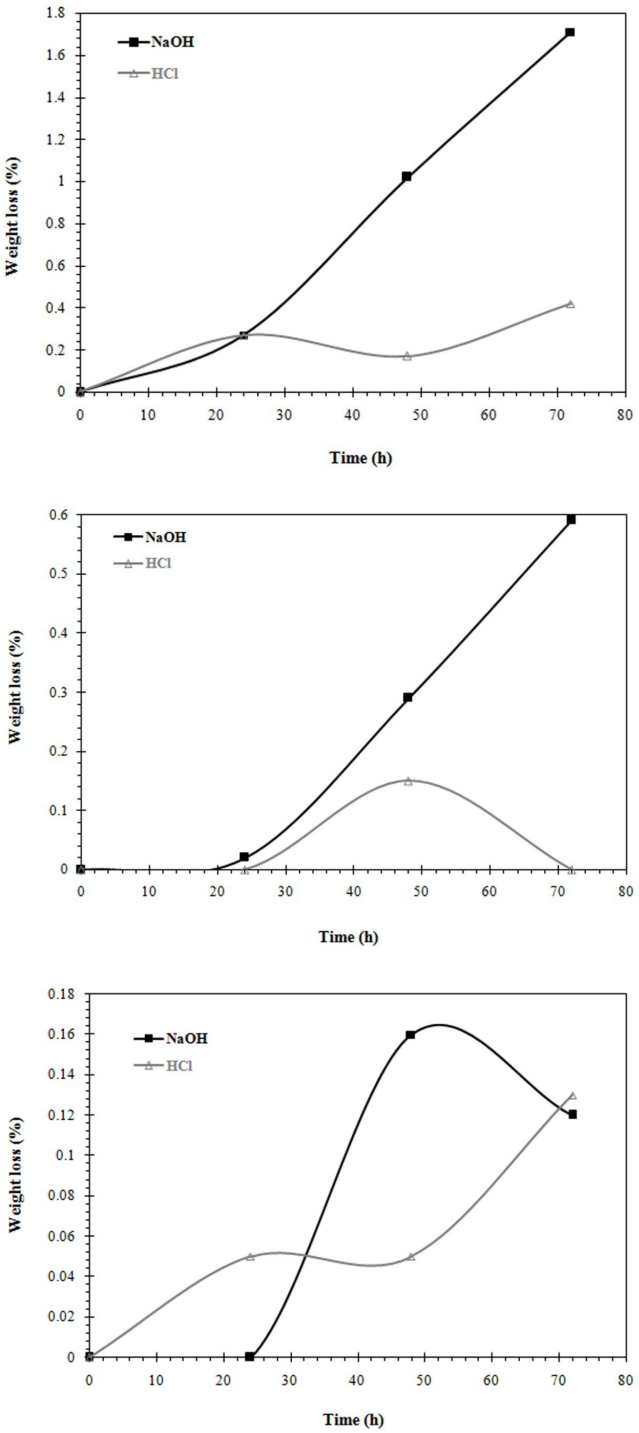

Fig. 7. Weight loss of zeolite support sintered at 850°C (a), 900°C (b) and 950°C (c) in HCl and NaOH as a function of time.

3.2.4. Porosity and mechanical measurements

Fig. 8 shows the evolution of the open porosity and the flexural strength of the zeolite support vs. sintering temperature. It is clear that the porosity decreases notably when the sintering temperature increases from 850°C to 950°C. This important decrease of the open porosity (from 46% to 37%) vs. sintering temperature could be explained by the occurrence of a sintering densification. This result is in agreement with other porous ceramic supports [31,32]. The support sintered at 900°C/3 h has reached an open porosity of 43.7%, which represents a good support porosity (>40%).

Porosity measurements remain not sufficient to optimize the sintering temperature of the ceramic support. It is then necessary to lead a mechanical study according to the sintering

temperature. The mechanical resistance tests have been carried out by the three points bending method (Lloyd Instrument, AMETEK STC, France) to control the resistance of the support tube fired at different temperatures. The dimensions (length/width/thickness) of the samples have been 45 mm/12 mm/2 mm and the distance separating the two points has been 30 mm. The increase of the sintering temperature has been accompanied by a densification phenomenon and consequently an increase in the flexural strength (from 6.67 MPa at 850°C to 18.02 MPa at 950°C). The material sintered at 900°C has reached a flexural strength of 12.65 MPa, which represents a good support mechanical resistance.

The main properties of the zeolite support sintered at 850°C, 900°C and 950°C are summarized in Table 2. It is clear that the sample sintered at 900°C/3 h meets the requirements of ceramic supports (open porosity > 40% and mechanical resistance > 10 MPa) useful for MF applications. Consequently, the zeolite support sintered at 900°C has been analyzed wider. Pore size measurements have shown an average pore diameter of 0.55 μm.

3.2.5. Determination of water permeability

The tests have been realized on the support sintered at 900°C/3 h with a TMP between 0 and 1 bar at room temperature. The corresponding membrane area has been 1.727×10^{-3} m^2. Fig. 9 shows the variation of water flux permeability vs. working pressure of zeolite support sintered at 900°C and zeolite membrane sintered at 850°C. It can be noted that the increase of the applied pressure causes a linear increase of the water flux. The support permeability (L_p) has been equal to 1,218 L/h m^2 bar.

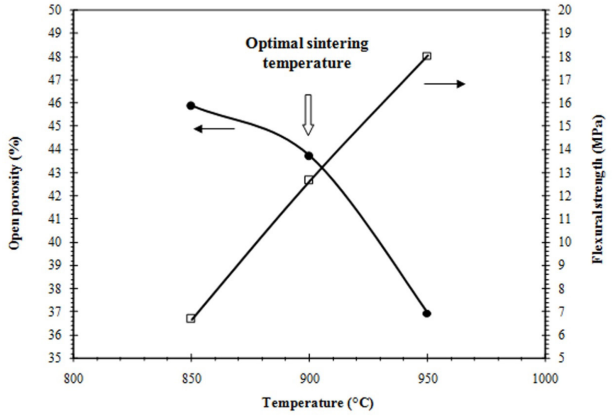

Fig. 8. Open porosity and flexural strength vs. sintering temperature of the zeolite support.

3.3. Characterization of the microfiltration membrane

3.3.1. Scanning electron microscopy

From cross-section SEM micrographs in Fig. 10 of zeolite membrane sintered at different temperatures, it is seen that there are no cracks and the adhesion between the support and the filtration layer is very good. This result confirms the good conditions of filtration layer deposition during the slip casting process. The thickness of the filtration layer is about 3.3, 2.2 and 2.8 μm for sintering temperature 820°C, 850°C and 880°C, respectively. The membrane surface micrographs seen in Fig. 11 show smooth and cracks-free surfaces with uniform pore distribution and particle size below 10 μm. The membrane sintered at 850°C with a thickness of about 2.2 μm (Fig. 11(b)) has been chosen for MF layer.

3.3.2. Pore size measurements

Pore size distribution of the membrane sintered at 850°C/3 h is shown in Fig. 12. The mean pore sizes of support and MF layer are 0.55 and 0.18 μm, respectively. This attribution is based on the comparison of distribution diagrams of both the support sintered at 900°C/3 h and the membrane sintered at 850°C/3 h. It is also clear that the pore size distribution of the filtration layer is narrower than that of the support.

3.3.3. Determination of membrane permeability

The tests have been realized on the membrane sintered at 850°C/3 h with a TMP between 1 and 3 bar at room

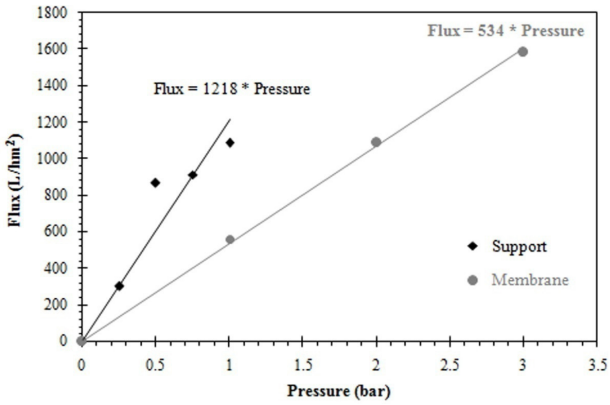

Fig. 9. Water flux permeability vs. working pressure of zeolite support sintered at 900°C and zeolite membrane sintered at 850°C.

Table 2
Properties of the zeolite support vs. sintering temperature

Sintering temperature (°C)	Weight loss after 72 h/HCl (%)	Weight loss after 72 h/NaOH (%)	Porosity (%)	Flexural strength (MPa)	Mean pore diameter (μm)	Water permeability (L/h m^2 bar)
850	0.42	1.71	45.85	6.67	–	–
900	*0*	*0.59*	*43.69*	*12.65*	*0.55*	*1,218*
950	0.13	0.12	36.94	18.02	–	–

Note: Italic values are correspond to optimal properties of the zeolite support.

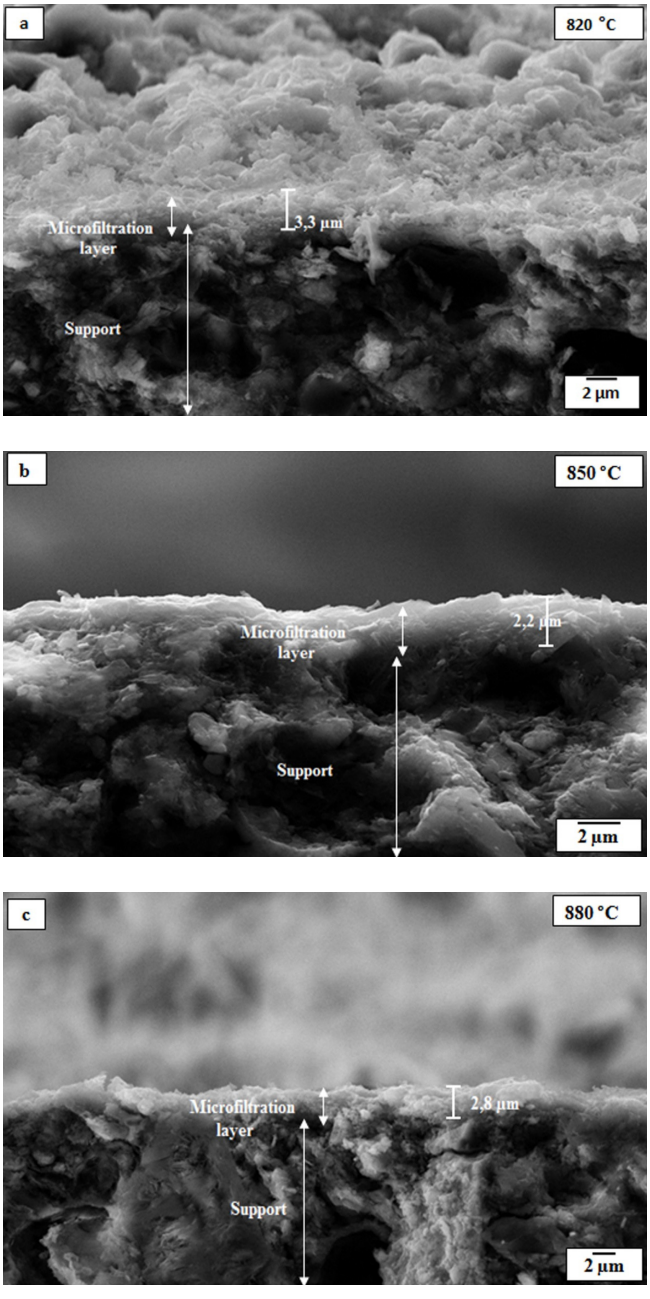

Fig. 10. SEM micrographs of tubular membrane cross-section sintered for 3 h at 820°C (a), 850°C (b) and 880°C (c).

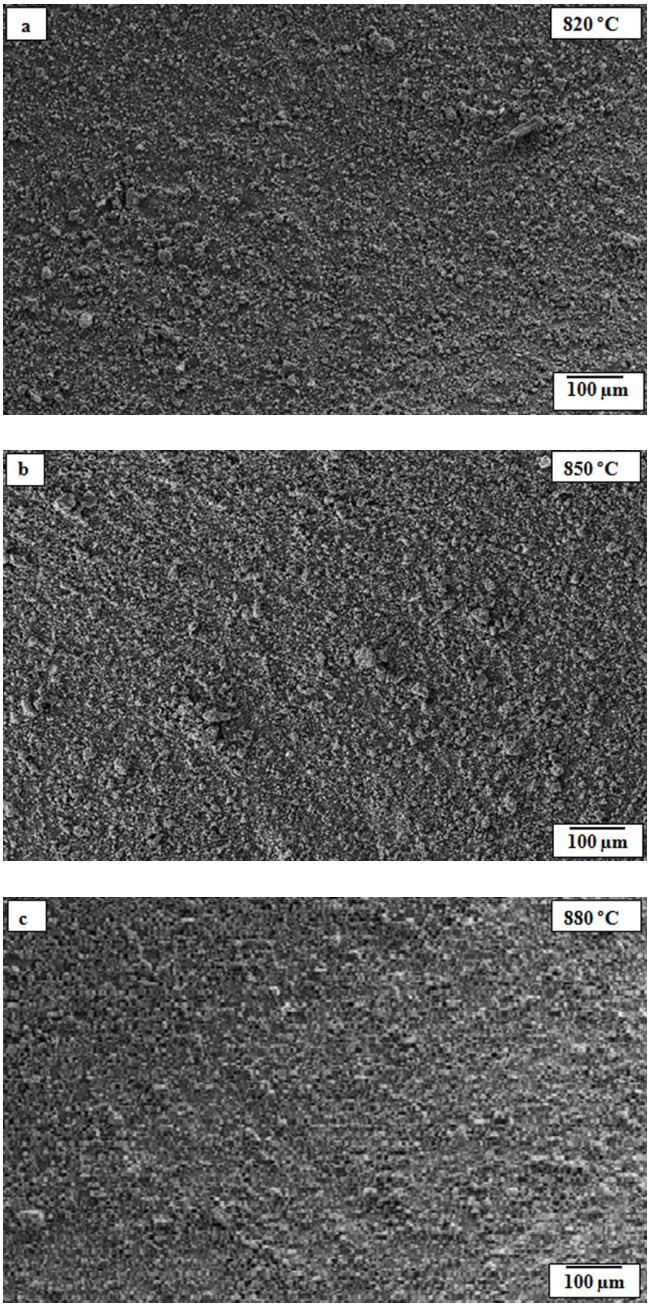

Fig. 11. SEM micrographs of tubular membrane surface sintered for 3 h at 820°C (a), 850°C (b) and 880°C (c).

temperature. It can be noted from Fig. 9 that the increase of the applied pressure causes a linear increase of the water flux. The same evolution is observed for both support and membrane. The water permeability of the membrane has been 534 L/h m^2 bar.

3.4. Application to the treatment of the cuttlefish effluents

The treatment of industrial wastewater can be achieved by membrane process. In this study, the MF membrane has been applied to the cuttlefish effluent produced from cuttlefish conditioning and freezing process. The tests of MF treatment have been carried out using an effluent obtained by dissolution of cuttlefish ink in a volume of distilled water. The filtration performances have been determined at room temperature and TMP of 1 bar. The evolution of the flux with time is given by Fig. 13. The flux decreases linearly during the first 20 min from 63 to 58 L/h m^2 and then stabilizes at 58 L/h m^2 beyond 20 min. This behavior could be explained by the formation of concentration polarization and fouling due to the interaction between membrane material and solution [33].

The main characteristics of the used effluent before and after MF treatment are illustrated in Table 3. It can be observed

that the chemical oxygen demand (COD) retention rate (COD achieved by a colorimetric method) has been superior to 57% and the turbidity determined by using a Turbidimeter (HACH RATIO 2100A) has been notably decreased. A total color removal has been obtained from 1 bar. These results confirm the important efficiency of the elaborated membrane in the treatment of cuttlefish effluent.

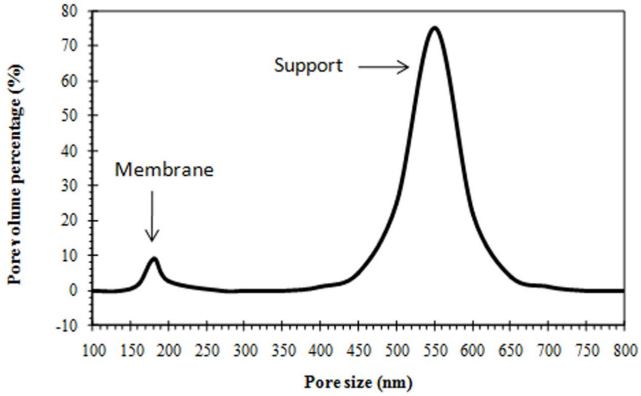

Fig. 12. Pore size distribution of zeolite membrane sintered at 850°C.

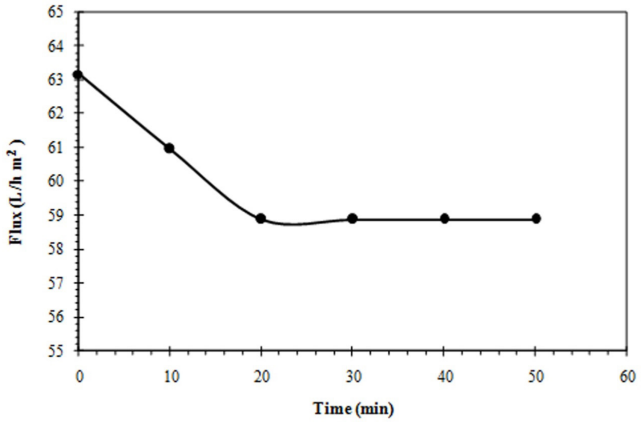

Fig. 13. Permeate flux vs. time of zeolite membrane sintered at 850°C (T = 25°C, TMP = 1 bar).

3.5. Comparative study

The results found in this work on Turkish zeolite are different compared with the other works relative to zeolite from China [20] and zeolite from Bulgaria [21]. In fact, Dong et al. [20] have fabricated zeolite multilayer MF membranes on tubular porous zeolite supports by dip-coating using natural zeolite from China as the starting material. The low cost obtained membranes could be used in prepurification of wastewater due to the good permeability and the pore structure. On the other hand, Hristov et al. [21] have fabricated low cost multilayer zeolite membranes on porous zeolite support by dip-coating process using natural zeolite from Bulgaria as the starting material. The good adhesion between the support and the layers allows the use of these zeolite membranes in several MF applications. It is so interesting to lead a comparative study concerning the main properties of the zeolite supports and the performances of the zeolite membranes. All the results are summarized in Table 4. It is clear that our Turkish zeolite support presents high properties in terms of mechanical resistance, porosity and chemical stability. On the other hand, the MF membrane obtained by slip casting method from only one zeolite filtration layer on Turkish zeolite support presents good performances, compared with Chinese zeolite and Bulgarian zeolite membranes with two filtration layers.

4. Conclusions

In this work, it has been shown that low cost MF membranes elaborated by slip casting process on tubular microporous Turkish zeolite supports (OD/ID = 8 mm/5 mm) may find MF application, such as the treatment of cuttlefish effluents. The obtained membrane at low sintering temperature

Table 3
Main characteristics of the effluent before and after filtration

	Raw effluent	Permeate (P = 1 bar)
pH	7.14	7.28
Conductivity (mS/cm)	1.3	1.31
Turbidity (NTU)	105	3.7
COD (mg/L)	425	180

Table 4
A comparative study concerning different zeolites

		Zeolite from Turkey (present work)	Zeolite from Bulgaria [21]	Zeolite from China [20]
Properties of supports sintered at 900°C	Porosity (%)	43.69	13.39	34.5
	Average pore size (μm)	0.55	–	5.86
	Mechanical resistance (MPa)	12.65	6	–
	Water permeate flux (L/h m² bar)	1,218	–	26,600
Properties of microfiltration membranes	Optimum firing temperature (°C)	850	800	900
	Number of layers	1	2	2
	Thickness (μm)	2.2	12	22
	Average pore size (μm)	0.18	0.5–0.3	0.54
	Water permeate flux (L/h m² bar)	534	–	3,200

(850°C/3 h) from non-expensive natural zeolite mineral has exhibited good adhesion between the support and the filtration layer, high quality of the surface, high porosity and an important efficiency in the treatment of cuttlefish effluent (decrease of turbidity, retention of COD and total color removal).

References

[1] Z. Cui, W. Peng, Y. Fan, W. Xing, N. Xu, Ceramic membrane filtration as seawater RO pre-treatment: influencing factors on the ceramic membrane flux and quality, Desal. Wat. Treat., 51 (2013) 2575–2583.

[2] J. Kujawa, W. Kujawski, S. Koter, K. Jarzynka, A. Rosicka, A. Larbo, Membrane distillation properties of TiO_2 ceramic membranes modified by perfluoroalkylsilanes, Desal. Wat. Treat., 51 (2013) 1352–1361.

[3] T.V. Gestel, C. Vandecasteele, A. Buekenhoudt, C. Dotremont, J. Luyten, R. Leysen, Alumina and titania multilayer membranes for nano-filtration: preparation, characterization and chemical stability, J. Membr. Sci., 207 (2002) 73–89.

[4] G.E. Romanos, T. Steriotis, A. Kikkinides, E.S. Kanellopoulos, N.K. Kasseelouri, Innovative methods for preparation and testing of Al_2O_3 supported silicalite-1 membranes, J. Eur. Ceram. Soc., 21 (2001) 119–126.

[5] A. Larbot, Fundamentals on inorganic membranes: present and new developments, Pol. J. Chem. Technol., 6 (2003) 8–13.

[6] L. Cot, A. Ayral, J. Durand, C. Guizard, N. Hovnanian, A. Julbe, A. Larbot, Inorganic membranes and solid state sciences, Solid State Sci., 2 (2000) 313–334.

[7] R.D. Colle, C.A. Fortulan, S.R. Fontes, Manufacture and characterization of ultra and micro-filtration ceramic membranes by isostatic pressing, Ceram. Int., 37 (2011) 1161–1168.

[8] M. Benito, M.J. Sanchez, P. Pena, M.A. Rodriguez, Development of a new high porosity ceramic membrane for the treatment of bilge water, Desalination, 214 (2007) 91–101.

[9] S. Khemakhem, A. Larbot, R. Ben Amar, New ceramic microfiltration membranes from Tunisian natural materials: application for the cuttlefish effluents treatment, Ceram. Int., 35 (2009) 55–61.

[10] N. Tahri, I. Jedidi, S. Cerneaux, M. Cretin, R. Ben Amar, Development of an asymmetric carbon microfiltration membrane: application to the treatment of industrial textile wastewater, Sep. Purif. Technol., 118 (2013) 179–187.

[11] M. Khemakhem, S. Khemakhem, S. Ayedi, R. Ben Amar, Study of ceramic ultra-filtration membrane support based on phosphate industry sub-product: application for the cuttlefish conditioning effluents treatment, Ceram. Int., 37 (2011) 3617–3625.

[12] I. Jedidi, S. Saïdi, S. Khemakhem, A. Larbot, N. Elloumi-Ammar, A. Fourati, A. Charfi, A. Ben Salah, R. Ben Amar, Elaboration of new ceramic microfiltration membranes from mineral coal fly ash applied to waste water treatment, J. Hazard. Mater., 172 (2009) 152–158.

[13] S. Ayadi, I. Jedidi, M. Rivallin, F. Gillot, S. Lacour, S. Cerneaux, M. Cretin, R. Ben Amar, Elaboration and characterization of new conductive porous graphite membranes for electrochemical advanced oxidation processes, J. Membr. Sci., 446 (2013) 42–49.

[14] F. Bouzerara, A. Harabi, S. Achour, A. Larbot, Porous ceramic supports for membranes prepared from kaolin and doloma mixtures, J. Eur. Ceram. Soc., 26 (2006) 1663–1671.

[15] N. Saffaj, M. Persin, S. Alami Younssi, A. Albizane, M. Cretin, A. Larbot, Elaboration and characterization of micro-filtration and ultra-filtration membranes deposited on raw support prepared from natural Moroccan clay: application to filtration of solution containing dye sand salts, Appl. Clay Sci., 31 (2006) 110–119.

[16] S. Khemakhem, R. Ben Amar, R. Ben Hassen, A. Larbot, A. Ben Salah, L. Cot, Fabrication of mineral supports of membranes for microfiltration/ultrafiltration from Tunisian clay, Ann. Chim. Sci. Mat., 31 (2006) 169–181.

[17] J. Cui, X. Zhang, H. Liu, S. Liu, K.L. Yeung, Preparation and application of zeolite/ceramic microfiltration membranes for treatment of oil contaminated water, J. Membr. Sci., 325 (2008) 420–426.

[18] T.F. Mastropietro, E. Drioli, S. Candamano, T. Poeriob, Crystallization and assembling of FAU nanozeolites on porous ceramic supports for zeolite membrane synthesis, Microporous Mesoporous Mater., 228 (2016) 141–146.

[19] M. Kazemimoghadam, T. Mohammadi, The pilot-scale pervaporation plant using tubular-type module with nano pore zeolite membrane, Desalination, 255 (2010) 196–200.

[20] Y. Dong, S. Chen, X. Zhang, J. Yang, X. Liu, G. Meng, Fabrication and characterization of low cost tubular mineral-based ceramic membranes for micro-filtration from natural zeolite, J. Membr. Sci., 281 (2006) 592–599.

[21] P. Hristov, A. Yoleva, S. Djambazov, I. Chukovska, D. Dimitrov, Preparation and characterization of porous ceramic membranes for micro-filtration from natural zeolite, J. Univ. Chem. Technol. Metall., 47 (2012) 476–480.

[22] F. Pechar, D. Rykl, Infrared spectra of natural zeolites of the stilbite group, Chem. Zvesti., 35 (1981) 189–202.

[23] M.M. Mohamed, F.I. Zidan, M. Thabet, Synthesis of ZSM-5 zeolite from rice husk ash: characterization and implications for photocatalytic degradation catalysts, Microporous Mesoporous Mater., 108 (2008) 193–203.

[24] I.O. Ali, M.S. Thabet, K.S. El-Nasser, A.M. Hassan, T.M. Salama, Synthesis of nanosized ZSM-5 zeolite from rice straw lignin as a template: surface-modified zeolite with quaternary ammonium cation for removal of chromium from aqueous solution, Microporous Mesoporous Mater., 160 (2012) 97–105.

[25] A. Charkha, M. Kazemeini, S.J. Ahmadi, H. Kazemian, Fabrication of granulated NaY zeolite nanoparticles using a new method and study the adsorption properties, Powder Technol., 231 (2012) 1–6.

[26] M. Asadollahi, D. Bastani, H. Kazemian, Permeation of single gases through TEG liquid membranes modified by Na-Y nano-zeolite particles, Sep. Purif. Technol., 76 (2010) 120–125.

[27] Y. Ma, C. Yan, A. Alshameri, X. Qiu, C. Zhou, D. Li, Synthesis and characterization of 13X zeolite from low-grade natural kaolin, Adv. Powder Technol., 25 (2014) 495–499.

[28] Y. Garcia-Basabe, I. Rodriguez-Iznaga, L.C.D. Menorval, P. Llewellyn, G. Maurin, D.W. Lewis, R. Binions, M. Autie, A.R. Ruiz-Salvador, Step-wise dealumination of natural clinoptilolite: structural and physicochemical characterization, Microporous Mesoporous Mater., 135 (2010) 187–196.

[29] A. Ates, C. Hardacre, The effect of various treatment conditions on natural zeolites: ion exchange, acidic, thermal and steam treatments, J. Colloid Interface Sci., 372 (2012) 130–140.

[30] A. Ates, Role of modification of natural zeolite in removal of manganese from aqueous solutions, Powder Technol., 264 (2014) 86–95.

[31] I. Jedidi, S. Khemakhem, A. Larbot, R. Ben Amar, Elaboration and characterization of fly ash based mineral supports for micro-filtration and ultra-filtration membranes, Ceram. Int., 35 (2009) 2747–2753.

[32] I. Jedidi, S. Khemakhem, S. Saïdi, A. Larbot, Preparation of a new ceramic micro-filtration membrane from mineral coal fly ash: application to the treatment of the textile dying effluents, Powder Technol., 208 (2011) 427–432.

[33] V. Chen, A.G. Fane, S. Maedani, I.G. Wenton, Particle deposition during membrane filtration of colloids: transition between concentration polarization and cake formation, J. Membr. Sci., 125 (1997) 109–122.